Supplementary Material

This Supplementary Material contains Figures S1-S8.

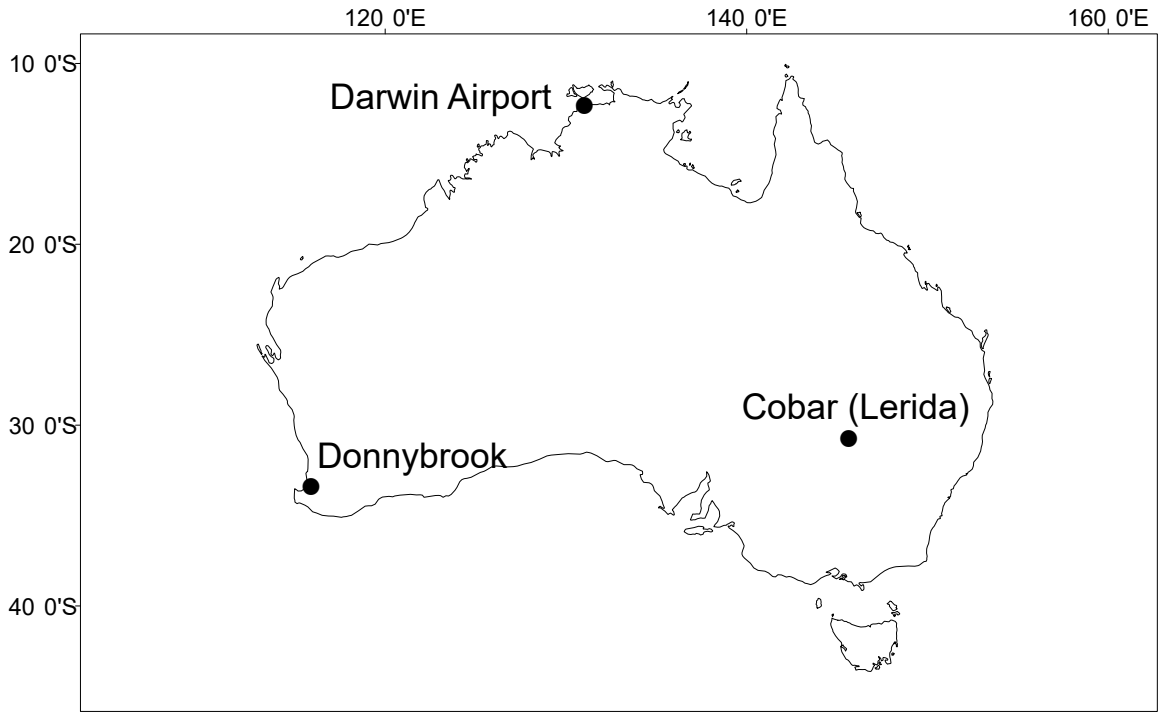

Figure S1. Location of precipitation observation sites used in this study.

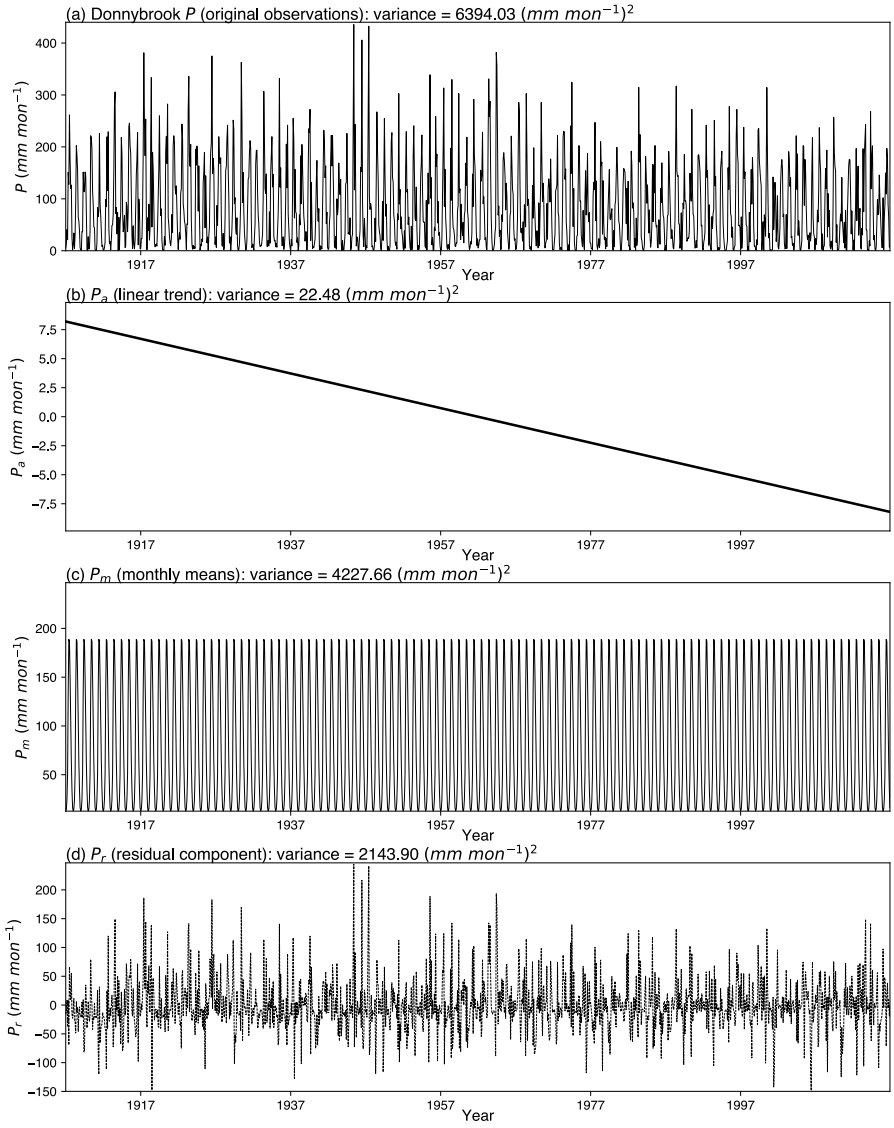

(e) Variance-covariance matrix (Unit: $(mm\ mon^{-1})^2$)

	P_a	P_m	P_r
P_a	22.48	-0.41	0.41
P_m	-0.41	4227.66	0.00
P_r	0.41	0.00	2143.90
Temporal variance of P : 6394.03			

*Note: The values along the diagonal of each line are variance values for three decomposed components, and other values are covariance values between the two crossed components.

Figure S2. Decomposition of monthly precipitation time series at Donnybrook (1907-2016) using linear trend removal. Panels show the (a) original observations (P), (b) linear trend (P_a), (c) monthly means (P_m), (d) residual random component (P_r) and the (e) variance-covariance matrix for the three components (P_a, P_m and P_r).

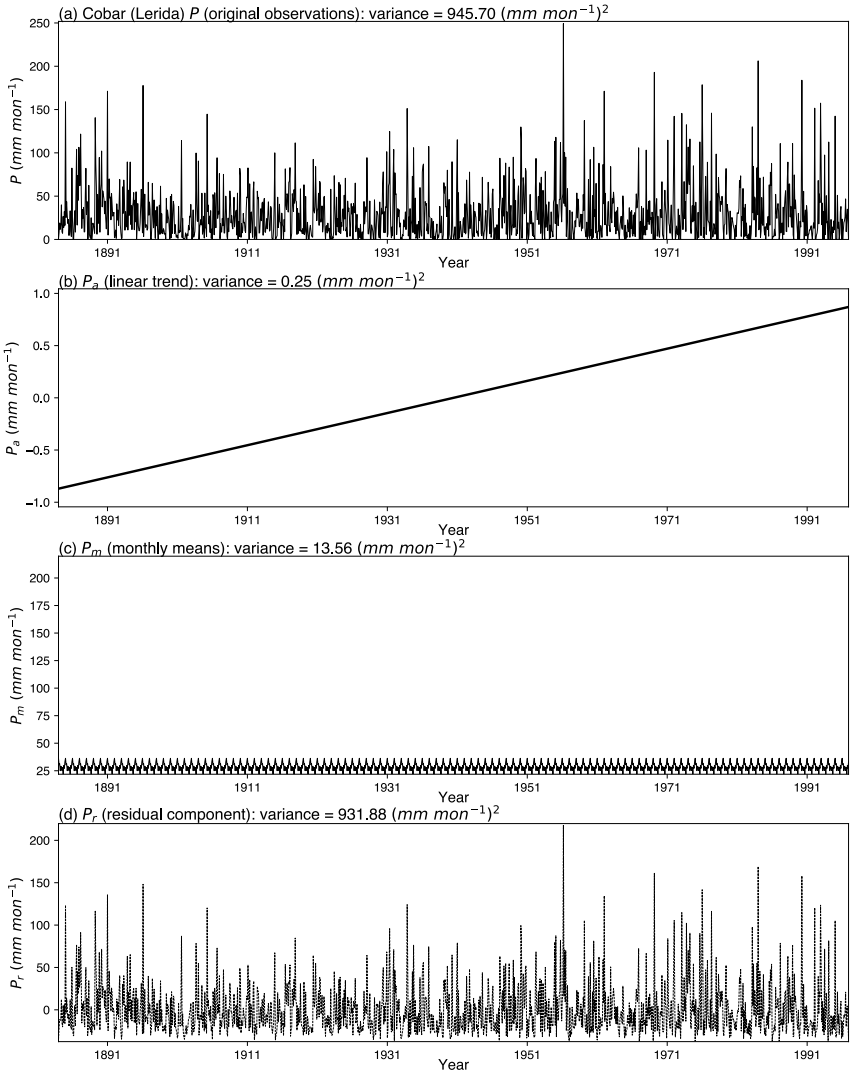

(e) Variance-covariance matrix (Unit: (*mm mon*$^{-1}$)^2)

	P_a	P_m	P_r
P_a	0.25	-0.01	0.01
P_m	-0.01	13.56	0.00
P_r	0.01	0.00	931.88
Temporal variance of P : 945.70			

*Note: The values along the diagonal of each line are variance values for three decomposed components, and other values are covariance values between the two crossed components.

Figure S3. Decomposition of monthly precipitation time series at Cobar (Lerida) (1884-1996) using linear trend removal. Panels show the (a) original observations (P), (b) linear trend (P_a), (c) monthly means (P_m), (d) residual random component (P_r) and the (e) variance-covariance matrix for the three components (P_a, P_m and P_r).

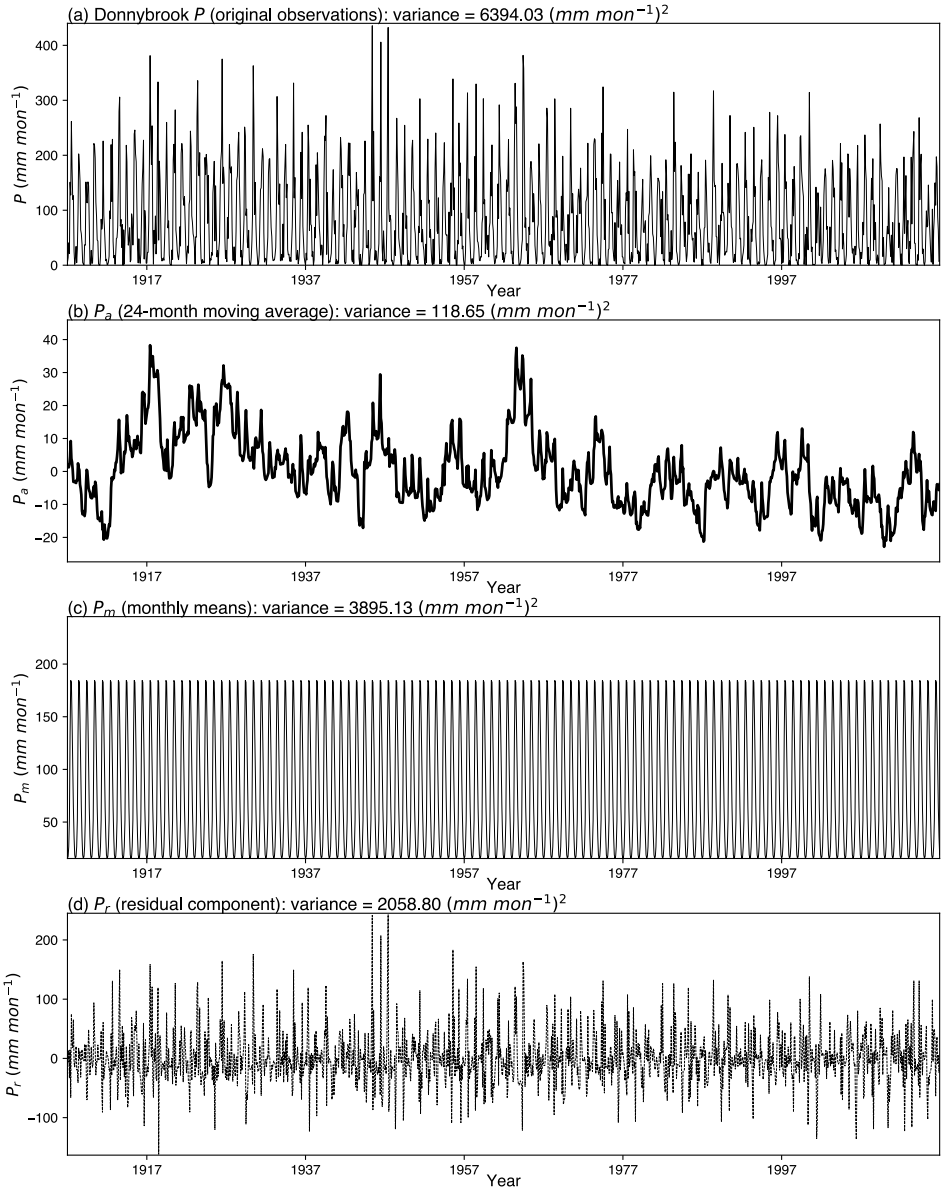

(e) Variance-covariance matrix (Unit: $(mm\ mon^{-1})^2$)

	P_a	P_m	P_r
P_a	118.65	162.47	-1.75
P_m	162.47	3895.13	0.00
P_r	-1.75	0.00	2058.80
Temporal variance of P : 6394.03			

*Note: The values along the diagonal of each line are variance values for three decomposed components, and other values are covariance values between the two crossed components.

Figure S4. Decomposition of monthly precipitation time series at Donnybrook (1907-2016) using 24-month moving average trend removal. Panels show the (a) original observations (P), (b) 24-month moving average trend (P_a), (c) monthly means (P_m), (d) residual random component (P_r) and the (e) variance-covariance matrix for the three components (P_a, P_m and P_r).

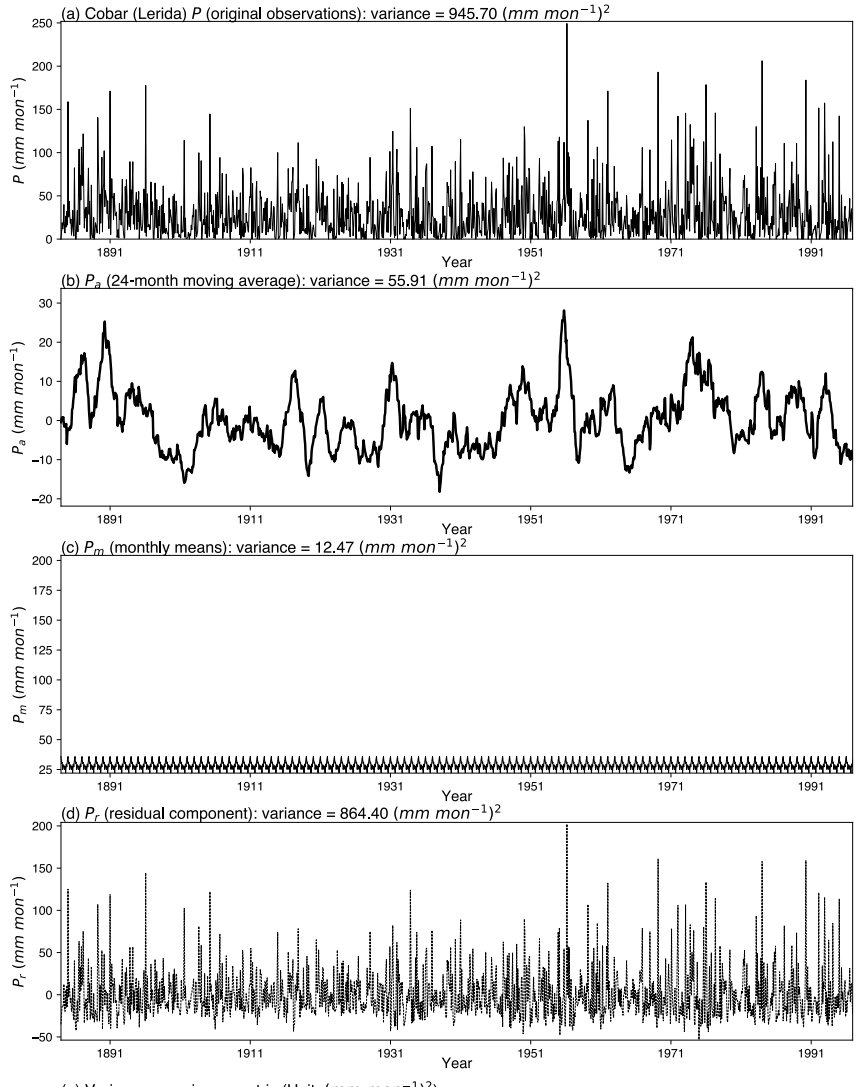

(e) Variance-covariance matrix (Unit: (mm mon^{-1})^2)

	P_a	P_m	P_r
P_a	55.91	0.53	5.93
P_m	0.53	12.47	0.00
P_r	5.93	0.00	864.40
Temporal variance of P : 945.70			

*Note: The values along the diagonal of each line are variance values for three decomposed components, and other values are covariance values between the two crossed components.

Figure S5. Decomposition of monthly precipitation time series at Cobar (Lerida) (1884-1996) using 24-month moving average trend removal. Panels show the (a) original observations (P), (b) 24-month moving average trend (P_a), (c) monthly means (P_m), (d) residual random component (P_r) and the (e) variance-covariance matrix for the three components (P_a, P_m and P_r).

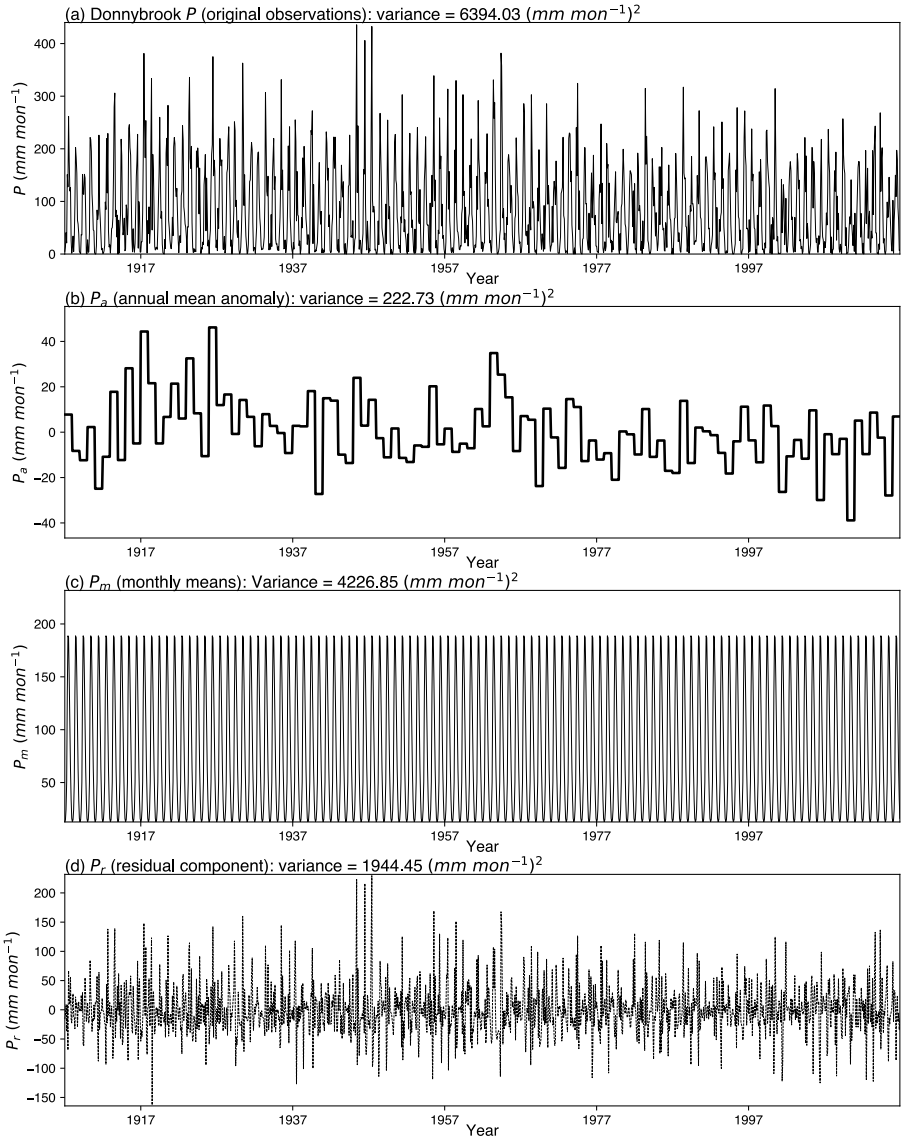

(e) Variance-covariance matrix (Unit: $(mm\ mon^{-1})^2$)

	P_a	P_m	P_r
P_a	222.73	0.00	0.00
P_m	0.00	4226.85	0.00
P_r	0.00	0.00	1944.45
Temporal variance of P : 6394.03			

*Note: The values along the diagonal of each line are variance values for three decomposed components, and other values are covariance values between the two crossed components.

Figure S6. Decomposition of monthly precipitation time series at Donnybrook (1907-2016) using the two-way ANOVA model. Panels show the (a) original observations (P), (b) annual anomaly (P_a), (c) monthly means (P_m), (d) residual random component (P_r) and the (e) variance-covariance matrix for the three components (P_a, P_m and P_r).

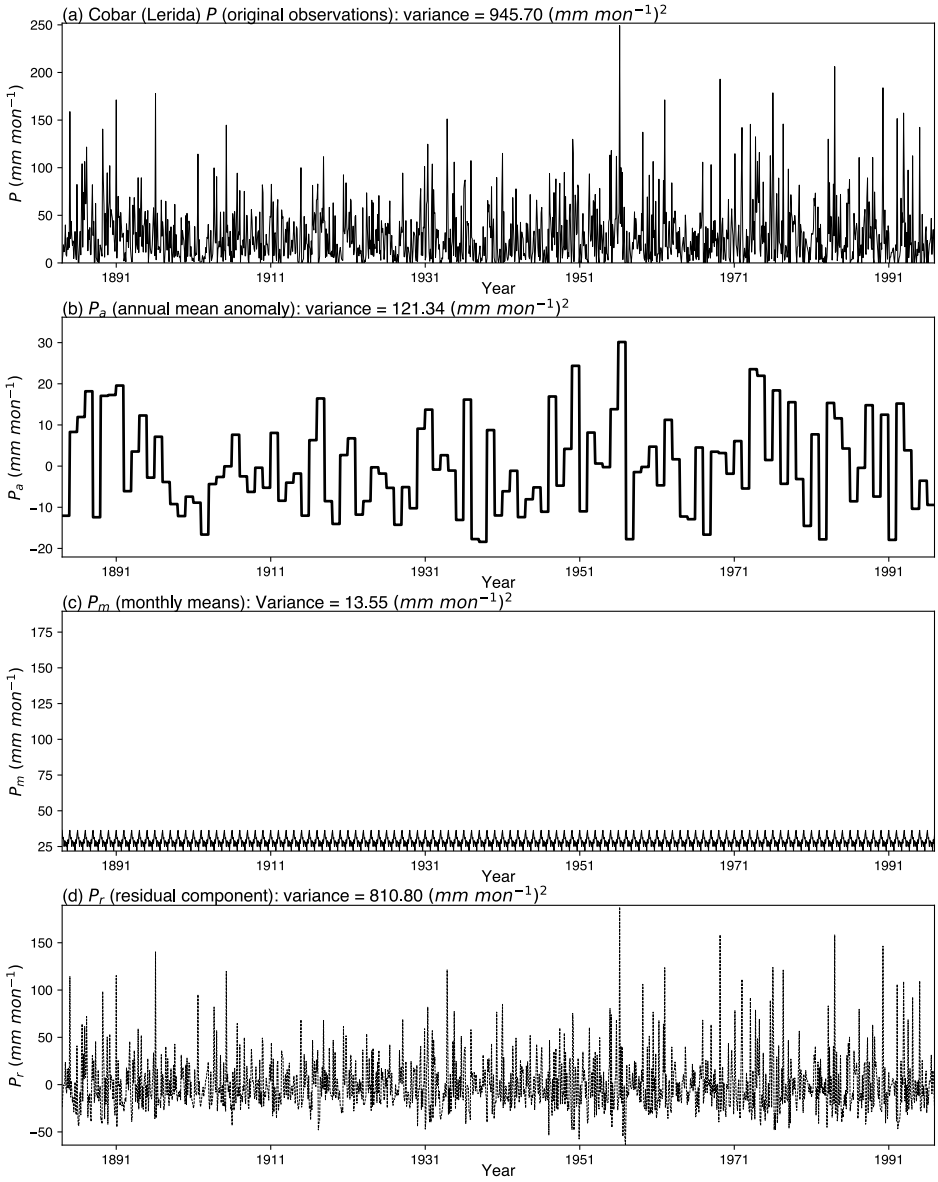

(e) Variance-covariance matrix (Unit: $(mm\ mon^{-1})^2$)

	P_a	P_m	P_r
P_a	121.34	0.00	0.00
P_m	0.00	13.55	0.00
P_r	0.00	0.00	810.80
Temporal variance of P : 945.70			

*Note: The values along the diagonal of each line are variance values for three decomposed components, and other values are covariance values between the two crossed components.

Figure S7. Decomposition of monthly precipitation time series at Cobar (Lerida) (1884-1996) using the two-way ANOVA model. Panels show the (a) original observations (P), (b) annual anomaly (P_a), (c) monthly means (P_m), (d) residual random component (P_r) and the (e) variance-covariance matrix for the three components (P_a, P_m and P_r).

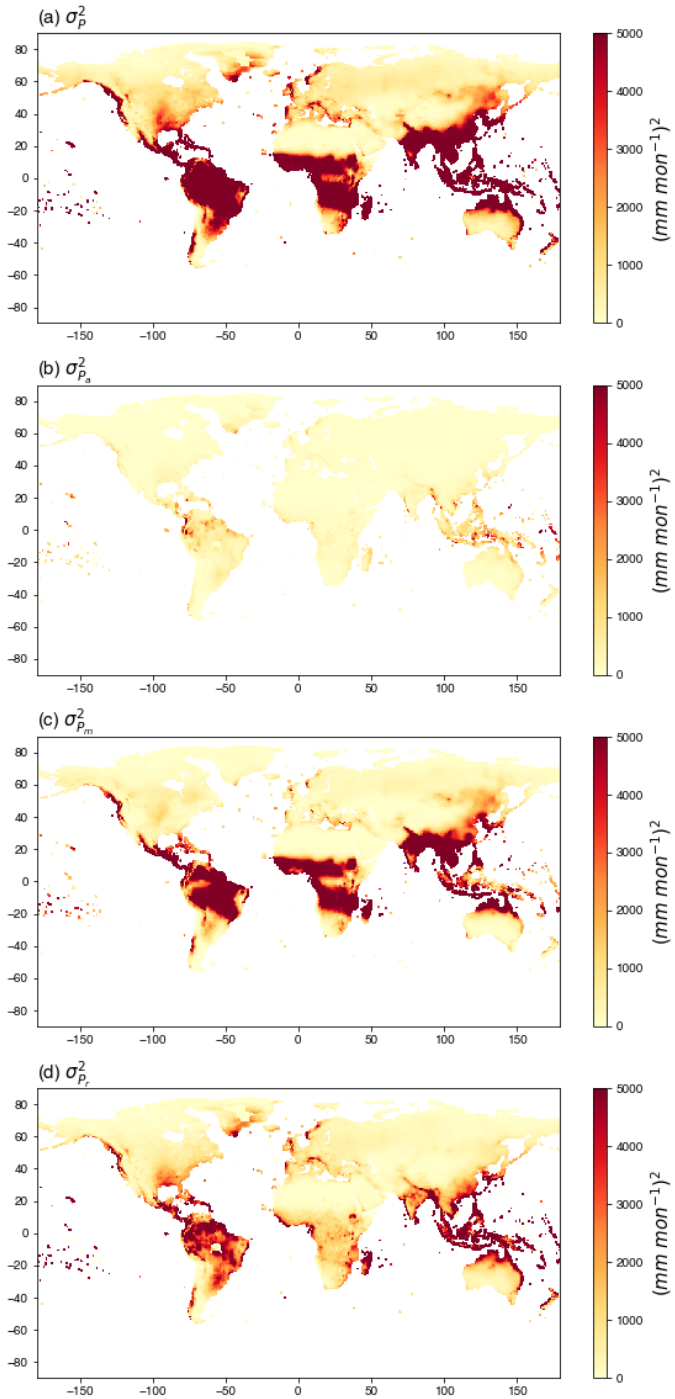

Figure S8. Temporal variance of global precipitation (a) σ^2_P, and variance of decomposed components, (b) annual anomaly $\sigma^2_{P_a}$, (c) monthly means $\sigma^2_{P_m}$ and (d) residual component $\sigma^2_{P_r}$ based on the two-way ANOVA model.